Pertanika J. Sci. & Technol. 31 (1): 351 - 372 (2023)

PERTANIKA JOURNALS

SCIENCE & TECHNOLOGY

Journal homepage: http://www.pertanika.upm.edu.my/

Optimization of the Formulation of Sago Starch Edible Coatings Incorporated with Nano Cellulose Fiber (CNF)

Rahmiyati Kasim[1], Nursigit Bintoro[1]*, Sri Rahayoe[1] and Yudi Pranoto[3]

[1]Department of Agricultural Engineering and Biosystem, Gadjah Mada University, 55281 Yogyakarta, Indonesia
[3]Department of Food and Agricultural Product Technology, Gadjah Mada University, 55281 Yogyakarta, Indonesia

ABSTRACT

This study aimed to produce new edible coatings based on the mixture of sago starch, cellulose nanofiber (CNF), glycerol, and tween-80.The effect of sago starch (5–10 g of starch/100 ml of distilled water), CNF (0.5–20% w/w), glycerol (10–30% w/w), and tween-80 (0.5–10% w/w) based on sago starch concentration on contact angle (CA), water vapor permeability (WVP), oxygen permeability (PO_2) and tensile strength (TS) properties of the edible coatings were optimized using factorial experimental design (2k).The result showed that the linear model for all independent variables was significant ($P<0.05$) on all responses (dependent variable).The sago starch concentration depicted a significant ($p < 0.001$) positive effect on contact angle; CNF showed a statistically significant effect on WVP, PO_2, and TS; tween-80 showed a significant effect on all dependent variables, whereas glycerol only affected WVP. The optimum concentrations of sago starch, CNF, glycerol, and tween-80 were predicted to be 5 g/100 ml distilled water, 20% w/w, 10% w/w, and 0.5% w/w based on sago starch, respectively to obtain the minimum contact angle, WVP, PO_2, and the maximum TS. The predicted data for the optimized coating formulation were in good agreement with the experimental value. This work revealed that the potential of sago starch/CNF based coating formulation could be effectively produced and successfully applied for coating of food.

Keywords: CNF, coatings, film, sago starch

ARTICLE INFO

Article history:
Received: 03 January 2022
Accepted: 18 April 2022
Published: 09 November 2022

DOI: https://doi.org/10.47836/pjst.31.1.21

E-mail addresses:
rahmiyatikasim@.ugm.ac.id (Rahmiyati Kasim)
nursigit@ugm.ac.id (Nursigit Bintoro)
yayoe_sri@yahoo.com (Sri Rahayoe)
pranoto@ugm.ac.id (Yudi Pranoto)
*Corresponding author

INTRODUCTION

The edible coating is a postharvest technology that can preserve fresh products by modifying the internal atmosphere of the fruit or vegetables by creating a semi-

ISSN: 0128-7680
e-ISSN: 2231-8526

permeable barrier to gases (O_2 and CO_2), moisture content, and movement of solids, consequently slowing the respiration rate and quality changes during storage (Deng et al., 2018). The effectiveness of edible coating in extending the shelf life of fruits and vegetables is determined, among others, by high barrier characteristics, suitable mechanical properties, high wettability, and good sensory qualities (Lopez-Polo et al., 2020; Sapper et al., 2019). The function and performance of the edible coating are influenced by the composition of the raw materials, the manufacturing process, and the method of application (Andrade et al., 2014).

Sago starch is a type of polysaccharide that has the potential to be used as material for making edible coatings because of its abundant availability, low cost, and higher productivity compared to other types of starch such as cassava starch, corn starch, and rice starch and contains high amylose approximately ± 28.84% (Karim & Tie, 2008; Zhu, 2019). Edible starch coatings have good gas barrier characteristics, produce a thin and transparent film, colorless and tasteless, and adhere well to the surface of fruit or vegetables (Punia et al., 2022; Thakur et al., 2019). However, the hydrophilic nature and high amylose content of starch cause the film or edible coating to be sensitive to high water content, thus affecting the water barrier properties and its mechanical properties become low, high water absorption (Shih & Zhao, 2021; Syafri et al., 2019) and low wettability coefficient of coating solution (Basiak et al., 2017). To overcome these, using cellulose nanofiller-reinforcement to the starch-based polymer has been confirmed as a new way for improving mechanical strength, gas permeability, and water barrier resistance properties (Bangar & Whiteside, 2021b; Shih & Zhao, 2021).

The development of edible coatings with the addition of nano reinforcement such as cellulose nanofiber (CNF) as a filler in a biopolymer matrix such as starch is very promising because it has good barrier properties, is small (diameter <100 nm) and uniform particle size, has high mechanical characteristics, water binding ability, has the same chemical structure as starch and is safe for health (Azeredo et al., 2017; Deng et al., 2017a). In recent years, CNF has been extensively studied and demonstrated to be effective to enhance the performance of biopolymer edible coatings/films such as chitosan (Ghosh et al., 2021), tapioca, potato and corn starch (Shih & Zhao, 2021), potato starch, tapioca starch, and chitosan (Gopi et al., 2019), banana starch (Tibolla et al., 2019), mango seed starch (Silva et al., 2019). Meanwhile, the addition of nano cellulose at high concentrations causes agglomeration in the coating solution.

Glycerol as a plasticizer is added to the starch coating and film to reduce the intermolecular forces of the polymer chains to reduce brittleness and increase the flexibility of films and coatings. However, the addition of glycerol (>33%) can increase water vapor permeability and decrease the mechanical characteristics of the film and coatings (Santacruz et al., 2015; Syafri et al., 2019; Thakur et al., 2019a). A surfactant (i.e. tween-80) is also

added to the coating material formula to increase the wettability and result in lower surface tension values (Santacruz et al., 2015). According to (Deng et al., 2017b), the addition of 10% (w/w dry basis) surfactant to the polymeric matric materials produced good wettability of coating formulation to the surface of fruits. Therefore, for the enhancement of functional properties of the coating, it is necessary to optimize the ingredients formula of coating.

To the best of our knowledge, no previous research has been conducted to prepare sago starch in combination with CNF or optimization of coating materials. The objective of this study was to optimize the coating material formula (sago starch, cellulose nanofiber (CNF), glycerol, and surfactant concentration) to produce an edible coating with low permeability value (WVP and O_2), low contact angle, and high tensile strength. In addition, this work would produce new information about the interaction between sago starch, CNF, glycerol, and surfactant concentrations on properties of coatings and films and produce a high-quality edible coating that is more environmentally friendly and competitive with wax coating materials.

MATERIALS AND METHODS

Materials

Sago starch produced by HD (HD Micro, Small and Medium Enterprises (MSME) Yogyakarta, Indonesia), 3% cellulose nanofiber (CNF) high fine slurry was obtained from the Process Development of the Maine University (ME, USA), mature green "Mas" bananas (Musa acuminata 'Lady Finger') fruits were harvested from a local farmer (Sleman, Yogyakarta, Indonesia), technical glycerol and distilled water purchased from Progo Mulyo CV (Yogyakarta, Indonesia), Tween-80 (Merck, Germany) obtained from Chemmix Pratama CV (Yogyakarta, Indonesia).

Preparation of Sago Starch and CNF Edible Coatings and Films

Sago starch and CNF nanocomposite edible coating were produced by the casting method according to the previous research method, with some modification (Balakrishnan et al., 2017; Meneguin et al., 2017; Tibolla et al., 2019; Widaningrum et al., 2015). Sago starch as a matrix (5–10 g) was diluted with 100 mL of distilled water while stirring at 700 RPM for 10 minutes at room temperature. Simultaneously, the CNF as a reinforcing agent (0.5–20% w/w) based on sago starch weight was dispersed in 50 ml of distilled water using a digital overhead stirrer (MULAB Type MS-40) at 700 RPM for 10 minutes. After that, the starch solution was added with the cellulose nanofiber (CNF) suspension, and the mixture was agitated by a digital overhead stirrer at 750 RPM for 20 minutes at room temperature. The mixture solution was then heated to 65°C and added tween-80 ($C_{64}H_{124}O_{26}$) as a surfactant material at varying concentrations (0.5–10% w/w of sago starch) while being stirred at a

speed of 750 RPM. After the temperature of the solution reaches 70°C, different amounts of glycerol ($C_3H_8O_3$) (10 - 30% w/w), based on sago starch weight, as the plasticizer, was added to the solution and continuously heated for 25 minutes while being stirred to obtain the film-forming and coating solutions. 60 ml of the coating solution at a temperature of 60°C was poured onto acrylic plates (20 cm x 20 cm) and dried at room temperature for 2–3 days. The concentrations were chosen based on preliminary experiments. The resulting film was stored for five days at room temperature before testing. For the measurement of the contact angle, it was done by applying the coating solution directly to the banana's peel then measured using a digital microscope.

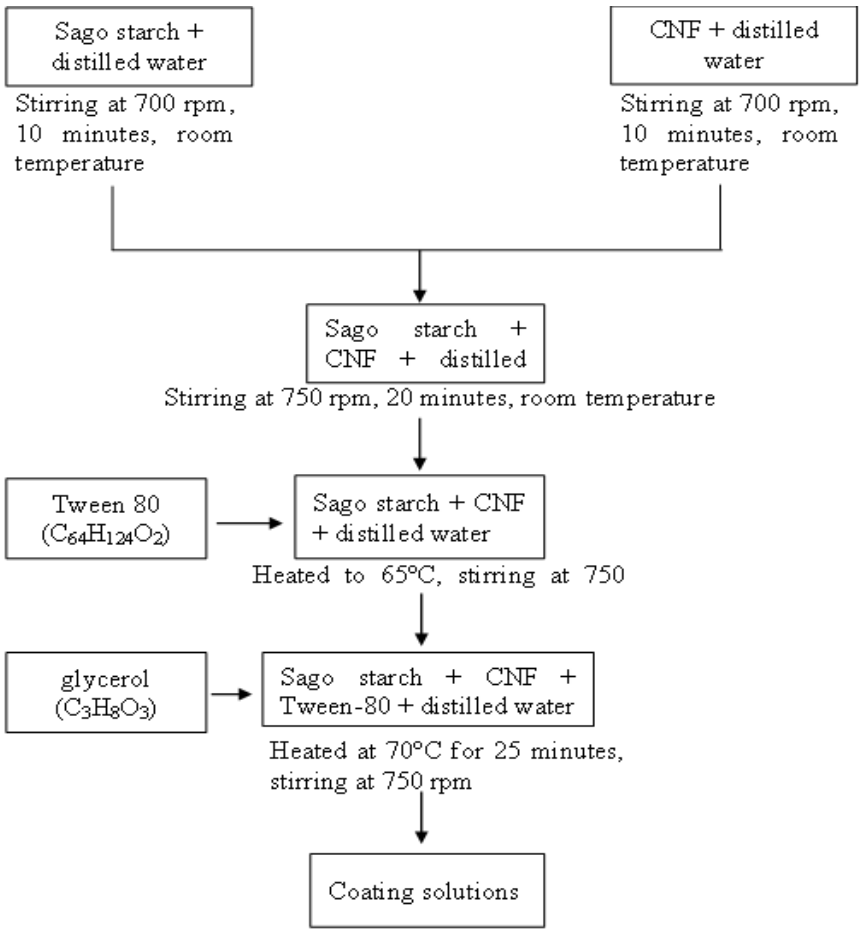

Figure 1. Schematic representation of preparation of sago starch (SS)-CNF nanocomposites

Characterization of the Coating and Film

Contact Angle (CA). The measurement of the contact angle is based on the method used by Deng et al. (2017b) and Rahayoe (2015). The coating solution was taken using a 500 µl syringe, then dripped from a height of 10 mm horizontally on the surface of a banana skin. After 30 seconds, the coating layer on the banana's peel was taken using a digital microscope (Dino-Lite AM2111 series). The results of these images were analyzed using Image J software to determine the contact angle between the droplets of the coating solution on the surface of banana skins. Measurement of contact angle was conducted at 3 points of each part of a banana's peel.

Water Vapor Permeability (WVP). The WVP of films was determined by the water desiccant method based on ASTM E 96 (1995). First, a circular-shaped edible film of 30 mm diameter was placed at the top of the WVP bottles containing 10 g of silica gel. Then, the WVP bottles were placed in a desiccator containing distilled water to produce RH 90 %. Finally, WVP bottles were weighed using an analytical balance (OHAUS) every hour for 8 hours of observation. As a result, the WVP is determined from Equations 1, 2, and 3, respectively:

$$\mathrm{WVT} = \frac{\left(\frac{G}{t}\right)}{A} \quad (1)$$

$$\mathrm{Permeance} = \frac{\mathrm{WVT}}{\Delta P} = \frac{\mathrm{WVT}}{S\,(R_1 - R_2)} \quad (2)$$

$$\mathrm{WVP} = \mathrm{Permeance\ x\ thickness} \quad (3)$$

Where WVT is the water vapor transmission rate (g/hour.m^2), G is the change in weight (from a straight line, g), t is time (hours), G/t = slope of a straight line (g/hour), A is the area of the mouth of the bottle (m^2), ΔP is the difference in water vapor pressure, mm Hg (1.333 x 10^2 Pa), S is the saturated vapor pressure at the test temperature, mm Hg (1.333 x 10^2 Pa), R_1 is the relative humidity in the bottles samples, while R_2 is the relative humidity of the environment, WVP is water vapor permeability (g/m s Pa).

Oxygen Permeability (PO_2). Permeability measurement of edible coating and film to oxygen was determined by the method proposed by Kubík and Zeman (2013) with slight modifications. The film to be tested was fixed between two acrylic chamber boxes with adhesive glue at the lips of the boxes. Then, the two chambers' boxes were fixed firmly using screws. The box was made from acrylic with the size of 15 x 15 x 15 cm with a hole at the base or the top of the boxes with a size 10 cm x 10 cm to regulate the initial oxygen concentration in the boxes. The upper chamber was filled with pure oxygen with a concentration of about 50–80%, while the bottom chamber was flushed using nitrogen

to lower oxygen concentration to around 18%. The changes in the oxygen concentration in the bottom box were measured every 10 minutes for 1.5 hours. Oxygen permeability is calculated according to the Equation 4 of Kubík and Zeman (2013) as follows:

$$P_x = \frac{\Delta\rho_p \, V \, M}{\Delta t \, S \, \rho_i^2 \, R \, T} \quad (4)$$

Where Px is the film permeability ($m^3/m^2.s.Pa$); ρ is the oxygen density in the bottom box (kg/m^3); ρ_i is the initial oxygen density in upper box (kg/m^3); M is the molecular weight mass of the oxygen (kg/mol); V is the volume of the chambers box (m^3); R is the universal gas constant 8314 (J/k mol K); T is the temperature (K); t is the time of the observation (s), and; S is the area of the film (m^2).

Film Thickness Measurement and Mechanical Properties. The film thickness was measured using a digital micrometer (Mitutoyo, Co., Code No.293–236, Japan) with an accuracy of ±0.001 mm. Measurements were taken from 8 different positions for each film sample (R. Thakur et al., 2018). The thickness measurement results are then averaged.

The tensile strength (TS) of the film was tested using the universal testing machine Zwick type Z0.5. The measurement method was based on (ASTM D882, 2010) with several method modifications from Cazón et al. (2018) and Ventura-Aguilar et al. (2018). The film was cut with a dumbbell with a size of 150 mm x 50 mm. Prior to measurements, the films were preconditioned at ±55% RH at 25°C in a desiccator containing sodium nitrate for five days. The measurement began with the film being clamped between the grips, with an initial distance between the grips being 50 mm at a speed of 10 mm/minute. Measurements were repeated two times for each sample. The value of tensile strength (MPa) of the film could be directly obtained from the measurement results.

Experimental Design and Optimization

In this study, a factorial experimental design (2k) was performed to assess the individual and combined effects of the main component of coating, namely the concentration of starch (X_1), CNF (X_2), glycerol (X_3), and tween-80 (X_4) on the contact angle, WVP, oxygen permeability (PO_2) and tensile strength, as responses variable. Construction of experimental factorial designs and data analysis was performed using Design Expert Software (Version 12.0.3.0, Stat-Ease Inc., Minneapolis, MN). The experimental design included different combinations of two levels (i.e., high (+1) and low levels (- 1)) of four independent variables and six additional replicates at the center point, leading to the 22 runs experimental design (Kania et al., 2021; Lavecchia et al., 2015). The minimum and maximum levels of each independent variable were determined based on recommendations from previous researchers (Deng et al., 2017a; Tibolla et al., 2019; Widaningrum et al., 2015).

The factors, levels, and responses values are presented in Table 1. To estimate the significance of the model, an analysis of variance (ANOVA) was undertaken with confidence levels higher than 95%. Pareto charts were also constructed to project the significance of factors X_1, X_2, X_3, and X_4 or the collective effect of factors; 3-D response surface plots were prepared to reveal the relationship and interactions between the four independent variables and responses. The optimization was based on the following combination: minimizing contact angle, WVP, PO_2, while maximizing TS. The numerical optimization to achieve the optimum concentrations of four independent variables (X_1: sago starch, X_2: CNF, X_3: glycerol, and X_4: tween-80) and to obtain the best nanocomposite coating/film properties including contact angle, WVP, PO_2, and TS were utilized. For validation of the regression models, the experimental data and fitted values predicted by the models were compared and percent error (PE) was calculated for each response.

RESULTS AND DISCUSSIONS

Interaction Effects of Coating Formulations on Contact Angle (CA)

In this study, the wettability of the coating was determined by the contact angle (ɵ) of the coating solution onto the banana skin surface. The value of CA of the coasting formulation on a banana epicarp in a range from 18.08° to 88.29° is shown in Table 1. It is noted that to gain the best coating; it is important to select a coating formulation with a low contact angle (ɵ) to generate closer to completely wetting, strong adhesion, weak cohesion, and a lipophilic condition (Andrade et al., 2014; Deng et al., 2017a).The significance of each model, independent variables, and interactions to the responses were evaluated based on the *p*-value, in which a *p*-value less than 0.05 was considered statistically significant (Kania et al., 2021). The analysis of variance (ANOVA) evaluation (Table 2) for CA showed the linear model term was significant (*p*-value < 0,005). In order to evaluate the goodness of fit of the model, different parameters including the coefficient of determination (R^2), the lack of fit F value, and the adequate precision were performed. In this study, the value of R^2 was 0.9384, the adequate precision was 20.4057 (< 4), and the lack of fit values was non-significant (*p*-value > 0,005), which indicate an adequate of the applied model and shows model can be used the prediction of contact angle of the coating solution. Moreover, Table 2 also represents that the contact angle of the coating formulation was influenced significantly (P < 0,005) by the linear effect of sago starch (X_1) and tween-80 (X_4) concentrations. However, CNF, glycerol levels and other combinations did not show a significant effect on contact angle value. The relation between and independent variables and the response can be expressed by Equation 5:

$$CA = 51{,}94 + 25{,}55\, X_1 - 6.51\, X_4 \quad (5)$$

Equation 5 shows that starch concentration had more influence than the tween-80 concentration on the contact angle, as the coefficients are 25.55 and 6.51, respectively. A positive coefficients value of the starch concentration means that the response (contact angle) is increased when the sago starch level increases.

The importance of significant main factors and interactions can be presented in the Pareto chart shown in Figure 2a. As shown in the Pareto chart, the factorial effects of very important main factors (above Bonferroni limit) were found to be in the following order: sago starch > tween-80. In order to show the combined effect of independent variables on the contact angle of the coating formulation, 3D response surfaces plots have been presented (Figure 2b). It was observed that the decline of contact angle was a function of starch and tween-80 concentration. The minimum amount of contact angle value could be observed at the low level of starch and higher tween-80 concentration (see Figure 2b). It may be associated with an increased contact angle as results of high starch concentration was due to an increase in viscosity of coating solution, which influences the amount of the materials adhered to the fruit surface and was difficult to spread on a solid surface (Soto-Muñoz et al., 2021; Soradech et al., 2017). Whereas, the addition of tween-80 resulted in a lower contact angle, probably due to it was might be caused by the humectant impact of surfactant and the hydrophobic chain of tween-80 could not interact with the polymers rich in polar groups; thus the film became hydrophilic (Stachowiak et al., 2020). In addition, several previous studies reported that surfactant diminished cohesion forces, hence decreasing the surface tension and increasing the wettability (Deng et al., 2017a; Riva et al., 2020; Sun et al., 2021).Thus, this surfactant improved compatibility between the solution and the fruit skin surface (Vieira et al., 2016). The lower contact angle indicated the higher interaction between coating solution and skin of surface, better hydrophilicity of the surface, and high degree wetting generates coating solution spreads easily on the fruit skin (Patil et al., 2021).

Table 1

The factorial experimental design (2^4) results

No	Run	Independent variables				Responses			
		Starch (% w/v)	CNF (% w/w)	Glycerol (% w/w)	Tween-80 (%w/w)	Contact Angle (°)	WVP $x10^{-11}$ (g/Pa s m)	PO_2 (cm^3/m^2. day Pa)	TS (MPa)
1	16	5 (-1)	0.5 (-1)	10 (-1)	0.5 (-1)	24.88	0.859	1314.77	23.15
2	15	10 (1)	0.5 (-1)	10 (-1)	0.5 (-1)	86.29	4.845	939.114	3.29
3	19	5 (-1)	20 (1)	10 (-1)	0.5 (-1)	35.44	0.607	745.268	25.56
4	2	10 (1)	20 (1)	10 (-1)	0.5 (-1)	88.29	1.032	982.803	26.65
5	18	5 (-1)	0.5 (-1)	30 (1)	0.5 (-1)	29.22	0.341	2228.03	10.38
6	26	10 (1)	0.5 (-1)	30 (1)	0.5 (-1)	87.66	1.090	2763.47	6.17

Table 1 *(Continue)*

No.	Run	Independent variables				Responses			
		Starch (% w/v)	CNF (% w/w)	Glycerol (% w/w)	Tween-80 (%w/w)	Contact Angle (°)	WVP x10^{-11} (g/Pa s m)	PO_2 (cm^3/m^2. day Pa)	TS (MPa)
7	30	5 (-1)	20 (1)	30 (1)	0.5 (-1)	30.41	0.653	4235.97	13.61
8	28	10 (1)	20 (1)	30 (1)	0.5 (-1)	85.38	1.797	786.182	6.05
9	10	5 (-1)	0.5 (-1)	10 (-1)	10 (1)	18.08	5.058	28769.9	2.36
10	4	10 (1)	0.5 (-1)	10 (-1)	10 (1)	66.58	5.651	21260.9	0.77
11	13	5 (-1)	20 (1)	10 (-1)	10 (1)	25.35	2.289	3181.23	3.66
12	11	10 (1)	20 (1)	10 (-1)	10 (1)	73.52	1.70 1	7503.29	9.08
13	14	5 (-1)	0.5 (-1)	30 (1)	10 (1)	19.08	3.504	4824.51	1.69
14	7	10 (1)	0.5 (-1)	30 (1)	10 (1)	69.53	2.902	24692	1.85
15	3	5 (-1)	20 (1)	30 (1)	10 (1)	28.65	0.534	2426.95	6.33
16	1	10 (1)	20 (1)	30 (1)	10 (1)	62.67	0.592	4011.19	12.13
17	27	7.5 (0)	10.25 (0)	20 (1)	5.25 (0)	29.68	0.587	8083.38	10.37
18	29	7.5 (0)	10.25 (0)	20 (1)	5.25 (0)	47.45	1.664	8899.55	5.19
19	5	7.5 (0)	10.25 (0)	20 (1)	5.25 (0)	61.73	0.312	5637.9	14.39
20	8	7.5 (0)	10.25 (0)	20 (1)	5.25 (0)	49.27	1.944	6582.57	18.55
21	6	7.5 (0)	10.25 (0)	20 (1)	5.25 (0)	49.27	0.214	5009.85	11.15
22	22	7.5 (0)	10.25 (0)	20 (1)	5.25 (0)	50.96	0.652	15539.1	12.95

Table 2

Significance level (P) calculated for investigating the effect of sago starch (X_1), CNF (X_2) glycerol (X_3), and tween-80 concentration (X4) into composite coatings and films the model fitting

Independent Variable	CA	WVP	PO_2	TS
Model Linear	<0.0001*	0.0025*	0.0075*	0.0121*
X_1 (starch)	<0.0001*	0.0642 ns	0.3737 ns	0.2423ns
X_2 (CNF)	0.524ns	0.0005*	0.0046*	0.0117*
X_3 (glycerol)	0.893ns	0.0042*	0.2796ns	0.0582ns
X_4 (tween-80)	0.010*	0.0035*	0.0009*	0.0016*
X_1X_2	0.518 ns	0.2072 ns	0.5598 ns	0.1029
X_1X_3	0.766 ns	0.2870 ns	0.2128 ns	0.5942 ns
X_1X_4	0.312 ns	0.0343*	0.2233 ns	0.0397 *
X_2X_3	0.570 ns	0.0413*	0.3279 ns	0.3220 ns
X_2X_4	0.900 ns	0.0104*	0.0050*	0.7975 ns
X_3X_4	0.974 ns	0.2051 ns	0.0930 ns	0.0183*

Table 2 *(Continue)*

Independent Variable	CA	WVP	PO_2	TS
$X_1X_2X_3$	0.801 ^{ns}	0.0631 ^{ns}	0.0638 ^{ns}	0.1573 ^{ns}
$X_2X_3X_4$	0.901 ^{ns}	0.2118 ^{ns}	0.1280 ^{ns}	0.1272 ^{ns}
R^2	0.9384	0.9282	0.9030	0.8888
Adjusted R^2	0.9276	0.8205	0.7576	0.7220
Adequate Precession	20.4057	10.8625	8.7020	8.6262
Lack of fit	0.9959 ^{ns}	0.6405 ^{ns}	0.3757 ^{ns}	0.6406^{ns}

Note. * Significant; ^{ns} Not significant

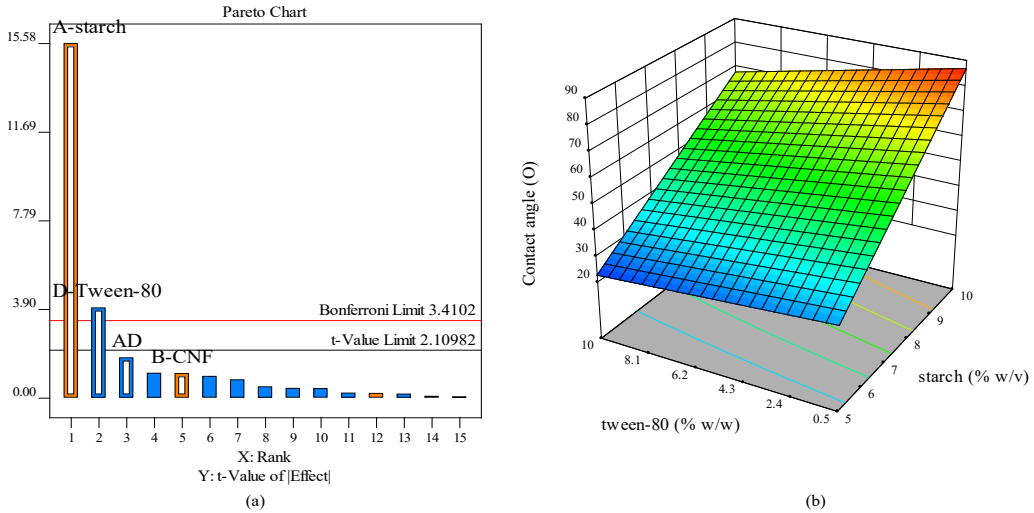

Figure 2. Analysis of (a) Pareto chart, (b) response surface of contact angle (CA) as a function of sago starch-tween-80

Interaction Effects of Coating Formulation on Water Vapor Permeability (WVP)

In the present study WVP values of the coating were in the range from 0.214 x 10^{-11} to 5.651 x 10^{-11} g/ Pa s m (Table 1). The model P-value of 0.0025 implies the linear model was significant (Table 2). As shown in Table 2, a high R^2 value ($R^2 > 85$) and close to the value of adjusted R^2 indicates that the model adequately represented the real relationship between the response and independent variables and is reliable for the prediction of WVP properties of the nanocomposite films and coatings as a function of tested variables (sago starch, CNF, glycerol and tween-80). The adequate precision value was greater than 4 (10.8625), and the lack of fit was non-significant (p = 0,6405) indicating an adequate signal and the model fit the test well with a small error. Furthermore, the statistical model reveals that WVP was affected significantly (95%) by the individual factor, namely CNF

concentration (X_2), glycerol concentration (X_3), tween-80 concentration (X_4), and by the interaction between factor (starch-tween 80 concentrations (X_1X_4), CNF-glycerol (X_2X_3), and CNF-tween 80 (X_2X_4). The relationship between responses (WVP) and independent variables was obtained as follows:

$$WVP\ (x10^{-11}) = 2.09 - 0.9403\,x_2 - 0.6644\,x_3 + 0.6880\,x_4 - 0.4278\,x_1x_4 + 0.4077\,x_2x_3 - 0.5596\,x_2x_4 \quad (6)$$

Equation 6 indicates that the CNF concentration had more impact than glycerol concentration on reduction of WVP, as coefficients are 0.9403 and 0.6644, respectively. Moreover, the value of positive coefficients of tween-80 concentration represents an increase of WVP. It is well known that better coating formulation had low WVP.

The factorial effects of very important main factors and their interactions were found to be in the following order: CNF > tween-80 > glycerol > CNF-tween > starch-tween > CNF-glycerol, as presented in the Pareto chart in Figure 3a. The evolution of WVP as a function of sago starch, CNF, glycerol, and tween-80 concentrations was presented in the 3D response surfaces plot in Figure 3b-d. It can be seen that the WVP value was reduction when CNF and glycerol concentrations were increased (Figure 3b and d), and the interaction starch of tween-80 (Figure 3b) was low concentration coating formulation. The lowest WVP ($0.214x10^{-11}$ g/Pa s m) was obtained in the coating formula with a composition of 7.5% (w/v) starch, 10.25% (w/w) CNF, 20% (w/w) glycerol, and 5.25% (w/w) tween-80. The WVP value in this study was lower when compared to previous studies, such as those reported by Soofi et al. (2021) in lemon waste powder film incorporated with 6% CNF ($1.12 \pm 0.09\times10^{-7}$ g/Pa h m or $3.11\pm 0.09\times10^{-11}$ g/Pa s m), Kim et al. (2021) in films based on TEMPO-oxidized CNF and sodium carboxymethyl cellulose (CMC) (0.77×10^{-9} g/Pa s m) & Yuan and Chen. (2021) in the corn starch-nanocellulose composite films ($4.41\ x10^{-4}$ g/Pa h m or $1.22\ x10^{-7}$ g/Pa s m). It indicates that the coating formulation in this study has an excellent barrier of water vapor.

The effect of reducing WVP as a result of added CNF on composite films and coating can be related to the following reasons: (1) The shape of cellulose fibers reduces the free space in the polymer matrix, obstructing the passage of water vapor through the surface film. Furthermore. nanocellulose interfaced with the glycerol in the film acts as a water vapor barrier (Da Silva et al., 2015). (2) The reduction in free hydrophilic groups (OH) and the matrix cohesiveness as a result of the formation of hydrogen bonds between CNF and biopolymer matrix implies a strong interaction between CNF and biopolymer matrix (Da Silva et al., 2015; Soofi et al., 2021). (3) The CNF leads to the formation of the long and zigzag pathways and acts as an obstacle to the extent of the diffusion path of water vapor transmission rate through the surface of the film (Bagheri et al., 2019; Paula et al., 2019; Soofi et al., 2021). (4) The CNF filling of void spaces between biopolymer chains reduces the mobility of chains. consequently decreasing the diffusion rate of water molecules and resulting in lower permeability (Bagheri et al., 2019; Soofi et al., 2021). (5) The high

crystalline properties of CNF restricted the passage of water vapor, resulting in a slower diffusion process and lower permeability (Xu et al., 2019). Likewise, in our, work increased glycerol in the starch and CNF composite film formulation decreased WVP. It may be due to the reduced density of the starch matrix, slow crystallization kinetics, and low glass transition temperature as a result of increased glycerol content in starch film (Thakur et al., 2019a). According to Da Silva et al. (2015), nano cellulose combined with glycerol acts as a barrier, thereby reducing water vapor permeability. Similar observations were reported by Thakur et al. (2019a), who indicated that the WVP value diminished at 20% (w/w of total starch) glycerol concentrations, but increased at 40% (w/w of total starch). Tween-80 has a HLB number of 15, indicating that it is readily soluble in water. Hydrophilic part of the tween-80 contributes to the increasing in WVP (Maniglia et al., 2019).

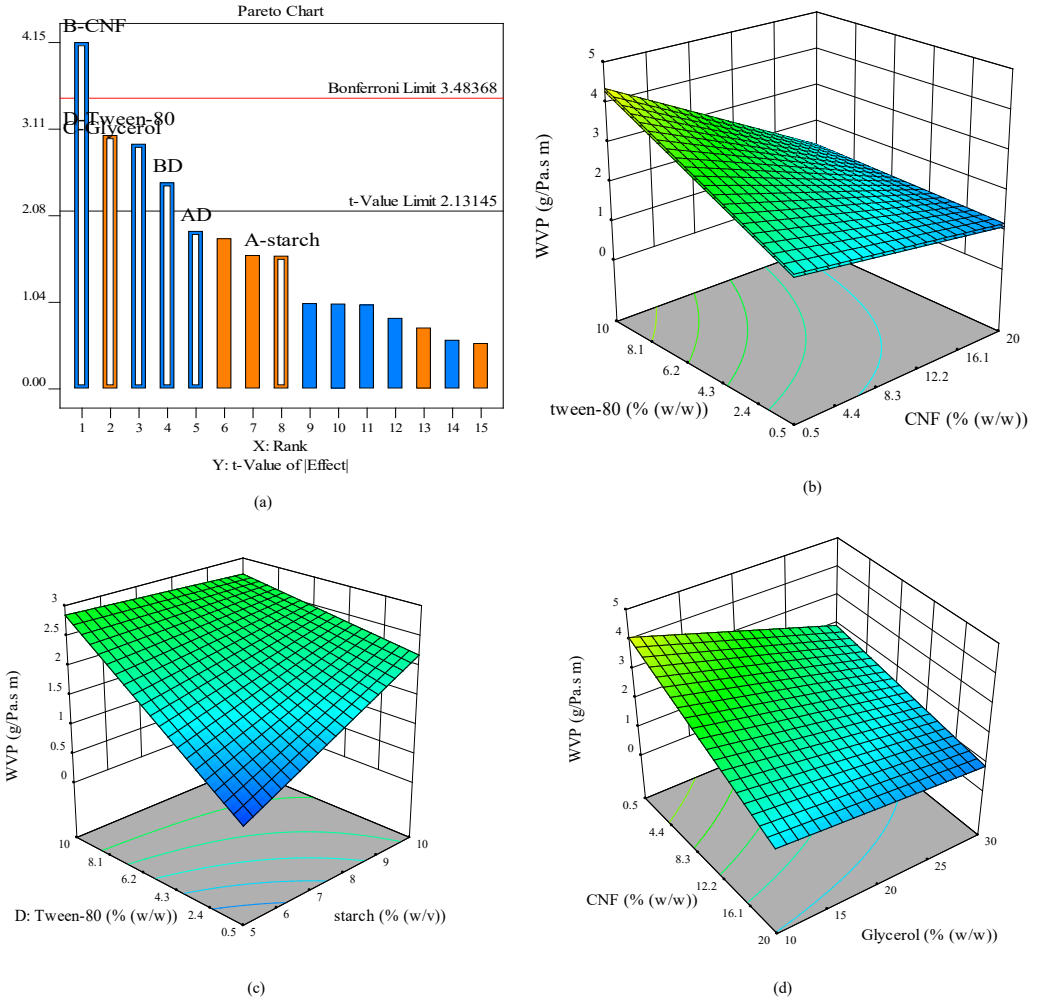

Figure 3. Analysis of (a) Pareto chart, (b) response surface of WVP as a function of CNF-tween-80, (c) starch-tween-80, and (d) CNF-glycerol concentration

Interaction Effects of Coating Formulation on Oxygen Permeability

Table 1 shows oxygen permeability changes with variation of formulation of coating. As can be seen from Table 2 for the PO_2, the p-value of less than 0.05 shows linear terms is acceptable (significant). Moreover, the high determination coefficients (R^2) value (>85%), the "adeq. Precision" more than 4, and a non-significant lack of fit indicate that the model can be used to navigate the design space. The factors, namely CNF (X_2), tween-80 (X_4) concentration, and interaction of these factors (X_2, X_4) are statistically significant to the model (p-value ≤ 0.05), while the remaining factors are not significant. Linear equation of the oxygen permeability as a function of factors of CNF(X_2), and tween-80 (X_4) is given by Equation 7:

$$PO_2 = 6916.60 - 3932.49\,X_2 + 5167.15\,X_4 - 3870.60\,X_2X_4 \quad (7)$$

The value of negative coefficients of CNF (Equation7) represents that low PO_2 can be achieved by using a high concentration of CNF.

The factorial effects of the main important factors and their interactions were found to be in the following order: tween-80> CNF >CNF-tween-80, as presented in the Pareto chart in Figure 4(b). In order to visualize the effect of interactions of independent variables on PO_2, 3D response surface plots were depicted Figure 4. In general. a decrease in PO_2 of edible films was obtained with the increases in CNF concentration and low concentration of tween-80 (Figure 4b). The lowest PO_2 (745.268 cm^3/m^2 day Pa = 0.0087 cm^3/m^2 s Pa) was reached at the highest of CNF (20% w/w) and lowest tween-80 concentration (0.5). PO_2 value in this work was lower than PO_2 (0.65 x 10^{13} cm^3/m s Pa) of corn starch film reported by Ribeiro et al., (2007). The fact that CNF has good oxygen barrier properties can be due to several reasons, as follows: (1) The dense network structure is formed by nanofibrils with more complexity, smaller pores, and more uniform particle size. Considering this fact, a complex, dense network increases the tortuosity for the diffusion of gases. Consequently, oxygen gas was compelled to diffuse through a more tortuous pathway throughout the film. It increases the time for the gas to navigate macroscopically throughout the film. thereby decreasing the permeability within the films. (2) The CNF films have higher entanglements within the film, which improve the tortuosity or extended the diffusion path; thereby, the oxygen molecules penetrate more slowly through the CNF films. (3) The high crystalline structure and a network structure held together via strong inter and intramolecular hydrogen bonds within the nanofibrils contribute to the gas barrier properties (Bangar & Whiteside. 2021a; Ferrer et al.. 2017; Siti Hajar et al.. 2021; Serpa & Vel. 2016). Furthermore, the present work has the same result as that reported by Ortega-toro et al. (2014), who found that PO_2 increased when surfactants were incorporated into the corn starch film. Whereas, the oxygen permeability is not much affected with the addition of varying the amount of plasticizer, as observed in previous works (Agarwal, 2021).

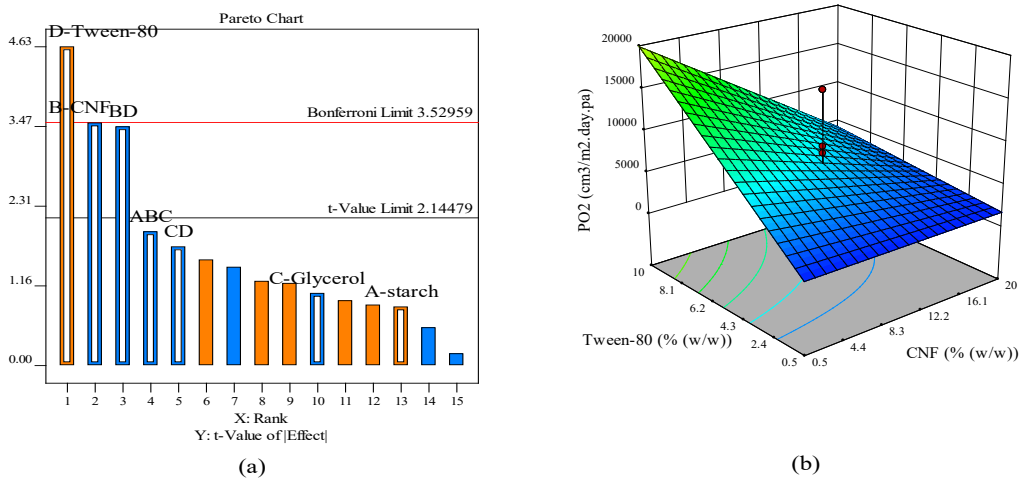

Figure 4. Analysis of (a) Pareto chart, (b) response surface of PO_2 as a function of CNF-tween-80

Interaction Effects of Coating Formulation on Tensile Strength

The result of the tensile strength test of varying formulas of the film (0.77 to 26.65 MPa) is displayed in Table 1. As observed in Table 2, it was found that p-values of tensile strength for the linear model were significant. The value of R^2 was 0.89, the adequate precision was 8.626 (< 4), and the lack of fit values was non-significant (*p*-value > 0,005), indicating adequate signal. It was also reported that the tensile strength of the composite film in the present study was significantly influenced by individual factors (CNF (X_2) and tween 80 concentration (X_4)) and combination by factors (starch-tween (X_1X_4) and glycerol-tween-80 (X_3X_4). The linear equations for tensile strength as a function of the four independent variables was given below (Equation 8):

$$TS = 9.55 + 3.34x_2 - 4.81\ x_4 + 2.52\ x_1x_4 \ + 3.04\ x_3x_4 \qquad (8)$$

The positive coefficients value of CNF concentration (3.34) in equation 8 indicated enhancement of TS. Whereas the value of the negative coefficient of tween-80 concentration showed diminished TS of starch film or coating.

As can be seen in the Pareto chart in Figure 5a, the factorial effects of very important main factors and their interactions (above Bonferroni limit) were found to be in the following order: tween-80 > CNF > glycerol-tween > starch-tween-80. The 3D response surface in Figure 5b-c depicts that the addition of 5–20% CNF significantly improved TS (Figure 5b). A Similar result regarding the effect of CNF of TS has been described by previous authors (Li et al., 2018b; Xu et al. 2019). As can be seen in Figure 5c and d, the opposite effect was observed with the addition of tween-80, which reduced

TS value obviously at all starch concentrations and high CNF concentration, respectively. Several past studies supported this result (Li et al., 2018a; Xu et al.. 2019). The highest TS value (26.65 MPa) in our work was obtained at high CNF concentration (20%) and low Tween 80 (0.5) in sago starch film/coating formulation (Table 1). TS value in this work was higher than that reported by a previous study (Shih & Zhao., 2021) in the film of tapioca starch incorporated 20% CNF (24.32 MPa) and the film is based on potato starch with 10% CNF (19.13 MPa). Several reasons have been argued for increasing the TS value of film by CNF: 1. Similar chemical structures of CNF and starch lead to a strong interaction between CNF and sago starch through the intermolecular hydrogen reaction, and CNF can be uniformly dispersed in the starch matrix, causing the compatibility between starch and CNF and efficient stress transfer from matrix to CNF (Li et al. 2018; Soofi et al., 2021), TS of films is directly associated with dispersion, compatibility, and hydrogen bonding between starch and nano cellulose (Bangar & Whiteside, 2021a), 2. The presence of CNF in void spaces between polymer chains caused decreasing mobility of chain and related with the change of crystalline is and the high mechanical strength of CNF (Hajar et al., 2021; Soofi et al., 2021), 3. Nano-sized CNF promoted strong intermolecular force, resulting in the rigidity enhancement of the films and, therefore high TS (Siti Hajar et al., 2021). In addition, it could be related to that surfactant are small size molecules that could persist between starch chains, like glycerol, increasing even more chain mobility and enhancing the initial plastic effect. The higher hydrophile-lipophile balance (HLB) value of tween 80 could interact with glycerol or water, facilitating its presence between starch chains which weaken the intermolecular hydrogen bonding. Therefore, resulting in the decrease of mechanical properties (Rodriguez et al., 2006).

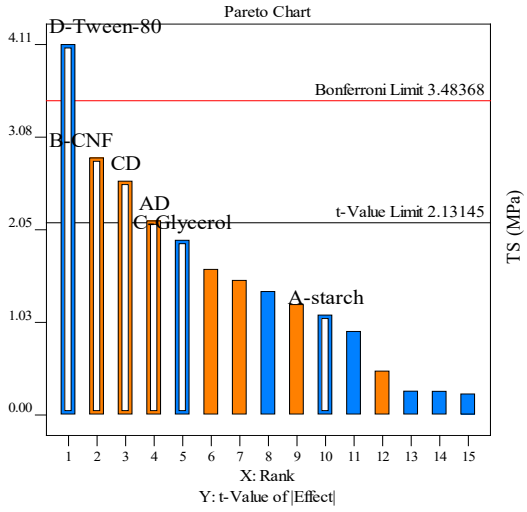

(a)

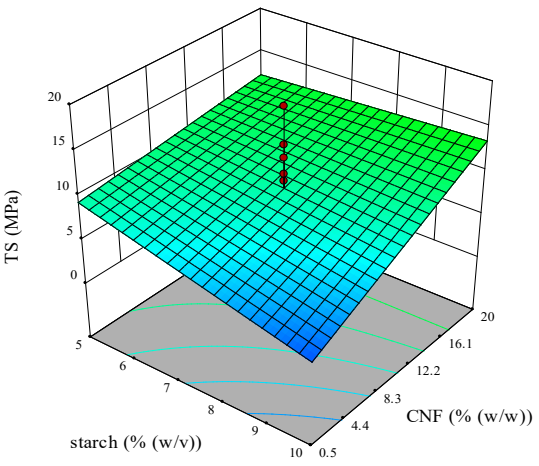

(b)

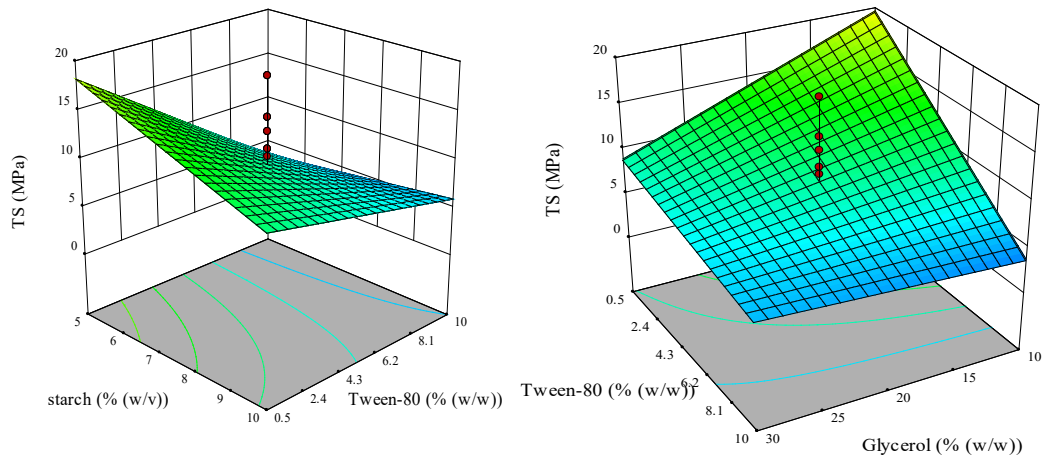

Figure 5. Analysis of (a) Pareto chart, (b) response surface of tensile strength as a function of starch-CNF, (c) starch-tween-80, and (d) tween-glycerol

Optimization of Coating Formulation

The optimization of the formulation of the coating solution was based on the four criteria: (1) minimizing contact angle; (2) minimizing water vapor permeability; (3) minimizing oxygen permeability; (4) maximizing tensile strength. Also, the importance value of 4 (++++) was selected for all criteria. The optimum concentration for producing the best characterization of starch and CNF coating was obtained with the addition of sago starch (5% w/v), CNF (20% w/w), and glycerol (10% w/w), and tween-80 (0.5% w/w) with maximum desirability 90%. The high desirability value in this work indicates that this formula is suitable for use.

Verification Experiments and Validation of the Model Equations

Verification experiments were conducted on the central points of the factorial design (7.5% w/v), CNF (10.25% w/w), glycerol (20% w/w), and tween-80 (5.25 % w/w) to validate the equations model adequacy and the result of film characterization compared to the predicted data. Table 3 shows the experimental and predicted value for the dependent variables at the center point. The percentage error (PE) was used for the evaluation of prediction accuracy. A small percentage error value indicated that the accuracy of response surface equations was better and the experimental values were close to the predicted values. From Table 3 it could be observed that the percentage error of the prediction equations differed according to the predicted parameters. The values of percentage error ranged from 8–15% with the smallest value was for WVP and the largest was for tensile strength. It meant that the most accurate prediction was for WVP with the percentage accuracy of around 92% and the least accurate was for tensile strength with the accuracy of around 85%.

Table 3
Predicted ad experimental data for the responses at optimum formulation

Responses	Predicted value	Experimental value	Percentage error (PE)
Contact Angle (°)	53.514	49.1	8.27
WVPx10^{-11} (g /s Pa m)	1.944	1.90	4.68
PO_2 (cm^3/m^2 day Pa)	6930.304	6763.966	11.147
Tensile strength (MPa)	11.147	9.68	15.18

CONCLUSION

The optimization of the coating formula was carried out to obtain the minimum value of the contact angle, oxygen permeability, water vapor permeability, and strong tensile strength. The value of contact angle depends on starch and tween-80 concentration. The reduction of WVP is influenced by the amount of CNF, glycerol, and tween-80. The addition of CNF in coating solution affects permeability (WVP and O_2) and tensile strength. The best film and coating characteristics were obtained in the formulation containing 5% (w/v) starch, 20% (w/w) CNF, 10% (w/w) glycerol, and 0.5% (w/w) tween-80. Verification model were performed on the central points of the factorial design (7.5% w/v), CNF (10.25% w/w), glycerol (20% w/w), and tween-80 (5.25 % w/w) resulted in the value contact angle (49.1°), WVP (1.90 x10^{-11} (g/s Pa m), PO_2 (6763.966 cm^3/m^2 day Pa), and TS (9.68 MPa) respectively.

ACKNOWLEDGEMENTS

The highest appreciation is given to the educational fund development institution (LPDP). Indonesia which has financed this research

REFERENCES

Agarwal, S. (2021). Major factors affecting the characteristics of starch based biopolymer films. *European Polymer Journal*, *160*, Article 110788. https://doi.org/10.1016/j.eurpolymj.2021.110788

Andrade, R., Skurtys, O., Osorio, F., Zuluaga, R., Gañán, P., & Castro, C. (2014). Wettability of gelatin coating formulations containing cellulose nanofibers on banana and eggplant epicarps. *LWT-Food Science and Technology*, *58*(1), 158-165. https://doi.org/10.1016/j.lwt.2014.02.034

ASTM D882. (2010). Standard test methods for tensile properties of thin plastic sheeting, *Annual Book of ASTM Standards*, *87*(Reapproved), 3-5. https://doi.org/10.1520/D0882-10

ASTM E 96 (1995). Standard test methods for water vapor transmission of materials. ASTM International. https://doi.org/10.1520/E0096-00E01

Azeredo, H. M. C., Rosa, M. F., Henrique, L., & Mattoso, C. (2017). Nanocellulose in bio-based food packaging applications. *Industrial Crops & Products*, *97*, 664-671. https://doi.org/10.1016/j.indcrop.2016.03.013

Bagheri, V., Ghanbarzadeh, B., Ayaseh, A., Ostadrahimi, A., Ehsani, A., Alizadeh-Sani, M., & Adun, P. A. (2019). The optimization of physico-mechanical properties of bionanocomposite films based on gluten/carboxymethyl cellulose/cellulose nanofiber using response surface methodology. *Polymer Testing*, *78*, Article 105989. https://doi.org/10.1016/j.polymertesting.2019.105989

Balakrishnan, P., Sreekala, M. S., Kunaver, M., Huskić, M., & Thomas, S. (2017). Morphology, transport characteristics and viscoelastic polymer chain confinement in nanocomposites based on thermoplastic potato starch and cellulose nanofibers from pineapple leaf. *Carbohydrate Polymers*, *169*, 176-188. https://doi.org/10.1016/j.carbpol.2017.04.017

Bangar, S. P., & Whiteside, W. S. (2021). Nano-cellulose reinforced starch bio composite films-A review on green composites. *International Journal of Biological Macromolecules*, *185*, 849-860. https://doi.org/10.1016/j.ijbiomac.2021.07.017

Basiak, E., Lenart, A., & Debeaufort, F. (2017). Effect of starch type on the physico-chemical properties of edible films. *International Journal of Biological Macromolecules*, *98*, 348-356. https://doi.org/10.1016/j.ijbiomac.2017.01.122

Cazón, P., Vázquez, M., & Velazquez, G. (2018). Novel composite films based on cellulose reinforced with chitosan and polyvinyl alcohol: Effect on mechanical properties and water vapour permeability. *Polymer Testing*, *69*, 536-544. https://doi.org/10.1016/j.polymertesting.2018.06.016

Da Silva, J. B. A., Nascimento, T., Costa, L. A. S., Pereira, F. V., Machado, B. A., Gomes, G. V. P., Assis, D. J., & Druzian, J. I. (2015). Effect of source and interaction with nanocellulose cassava starch, glycerol and the properties of films bionanocomposites. *Materials Today: Proceedings*, *2*(1), 200-207. https://doi.org/10.1016/j.matpr.2015.04.022

Deng, Z., Jung, J., Simonsen, J., & Zhao, Y. (2017). Cellulose nanomaterials emulsion coatings for controlling physiological activity, modifying surface morphology, and enhancing storability of postharvest bananas (*Musa acuminate*). *Food Chemistry*, *232*, 359-368. https://doi.org/10.1016/j.foodchem.2017.04.028

Deng, Z., Jung, J., Simonsen, J., & Zhao, Y. (2018). Cellulose nanocrystals pickering emulsion incorporated chitosan coatings for improving storability of postharvest bartlett pears (*Pyrus communis*) during long-term cold storage. *Food Hydrocolloids*, *84*, 229-237. https://doi.org/10.1016/j.foodhyd.2018.06.012

Ferrer, A., Pal, L., & Hubbe, M. (2017). Nanocellulose in packaging: Advances in barrier layer technologies. *Industrial Crops & Products*, *95*, 574-582. https://doi.org/10.1016/j.indcrop.2016.11.012

Ghosh, T., Nakano, K., & Katiyar, V. (2021). Curcumin doped functionalized cellulose nanofibers based edible chitosan coating on kiwifruits. *International Journal of Biological Macromolecules*, *184*, 936-945. https://doi.org/10.1016/j.ijbiomac.2021.06.098

Gopi, S., Amalraj, A., Jude, S., Thomas, S., & Guo, Q. (2019). Bionanocomposite films based on potato, tapioca starch and chitosan reinforced with cellulose nanofiber isolated from turmeric spent. *Journal of the Taiwan Institute of Chemical Engineers*, *96*, 664-671. https://doi.org/10.1016/j.jtice.2019.01.003

Hajar, O. S., Nordin, N., Ayuni, N., Azman, A., Sya, I., Amin, M., & Kadir, R. (2021). Effects of nanocellulose fi ber and thymol on mechanical, thermal, and barrier properties of corn starch films. *International Journal of Biological Macromolecules. 183*, 1352-1361. https://doi.org/10.1016/j.ijbiomac.2021.05.082

Kania, D., Yunus, R., Omar, R., Abdul, S., & Mohamed, B. (2021). Physicochemical and engineering aspects rheological investigation of synthetic-based drilling fluid containing non-ionic surfactant pentaerythritol ester using full factorial design. *Colloids and Surfaces A: Physicochemical and Engineering Aspects*, *625*, Article 126700. https://doi.org/10.1016/j.colsurfa.2021.126700

Karim, A. A., & Tie, A. P. (2008). Starch from the sago (*Metroxylon sagu*) palm tree - Properties, prospects, and challenges as a new industrial source for food. *Comprehensive Reviews in Food Science and Food Safety*, *7*(3), 215-228. https://doi.org/10.1111/j.1541-4337.2008.00042.x

Kim, H., Roy, S., & Rhim, J. (2021). Effects of various types of cellulose nanofibers on the physical properties of the CNF-based films. *Journal of Environmental Chemical Engineering*, *9*(5), Article 106043. https://doi.org/10.1016/j.jece.2021.106043

Kubík, Ľ., & Zeman, S. (2013). Determination of oxygen permeability of polyethylene and polypropylene nonwoven fabric foils. *Research in Agricultural Engineering, 59*(3), 105-113.

Lavecchia, R., Medici, F., Piga, L., & Zuorro, A. (2015). Factorial design analysis of the recovery of flavonoids from bilberry fruit by-products. *International Journal of Applied Engineering Research*, *10*(23), 43555-43559.

Li, M., Tian, X., Jin, R., & Li, D. (2018). Preparation and characterization of nanocomposite films containing starch and cellulose nanofibers. *Industrial Crops and Products*, *123*, 654-660. https://doi.org/10.1016/j.indcrop.2018.07.043

Lopez-Polo, J., Silva-Weiss, A., Zamorano, M., & Osorio, F. A. (2020). Humectability and physical properties of hydroxypropyl methylcellulose coatings with liposome-cellulose nanofibers: Food application. *Carbohydrate Polymers*, *231*, Article 115702. https://doi.org/10.1016/j.carbpol.2019.115702

Maniglia, B. C., Denise, Laroque, D. A., de Andrade, L. M., Carciofi, B. A. M., Tenorio, J. A. S., & de Andrade, C. J. (2019). Production of active cassava starch films; effect of adding a biosurfactant or synthetic surfactant. *Reactive and Functional Polymers, 144*, Article 104368. https://doi.org/10.1016/j.reactfunctpolym. 2019.104368

Meneguin, A. B., Ferreira Cury, B. S., dos Santos, A. M., Franco, D. F., Barud, H. S., & da Silva Filho, E. C. (2017). Resistant starch/pectin free-standing films reinforced with nanocellulose intended for colonic methotrexate release. *Carbohydrate Polymers*, *157*, 1013-1023. https://doi.org/10.1016/j.carbpol.2016.10.062

Ortega-toro, R., Jiménez, A., Talens, P., & Chiralt, A. (2014). Effect of the incorporation of surfactants on the physical properties of corn starch films. *Food Hydrocolloids*, *38*, 66-75. https://doi.org/10.1016/j.foodhyd.2013.11.011

Rodriguez, M., Oses, J., Ziani, K., & Mate, J. I. (2006). Combined effect of plasticizers and surfactants on the physical properties of starch based edible films. *Food Research International, 39*(8), 840-846. https://doi.org/10.1016/j.foodres.2006.04.002

Patil, S., Bharimalla, A. K., Mahapatra, A., Dhakane-Lad, J., Arputharaj, A., Kumar, M., Raja, A. S. M., & Kambli, N. (2021). Effect of polymer blending on mechanical and barrier properties of starch-polyvinyl alcohol based biodegradable composite films. *Food Bioscience*, *44*(Part A), Article 101352. https://doi.org/10.1016/j.fbio.2021.101352

Paula, A., Lamsal, B., Luiz, W., Magalhães, E., & Mottin, I. (2019). Cassava starch films reinforced with lignocellulose nanofibers from cassava bagasse. *International Journal of Biological Macromolecules*, *139*, 1151-1161. https://doi.org/10.1016/j.ijbiomac.2019. 08.115

Punia, S., Scott, W., Dunno, K. D., Armstrong, G., Dawson, P., & Love, R. (2022). Starch-based bio-nanocomposites films reinforced with cellulosic nanocrystals extracted from Kudzu (*Pueraria montana*) vine. *International Journal of Biological Macromolecules*, *203*, 350-360. https://doi.org/10.1016/j.ijbiomac.2022.01.133

Rahayoe, S. (2015). *Control of characteristics of chitosan film as fruit coating with the variation of types and additive compositions in making coating solutions* (Doctoral dissertation). Gadjah Mada University, Indonesia. https://lib.ugm.ac.id/

Ribeiro, C., Vicente, A. A., Teixeira, J. A., & Miranda, C. (2007). Optimization of edible coating composition to retard strawberry fruit senescence. *Postharvest Biology and Technology*, *44*(1), 63-70. https://doi.org/10.1016/j.postharvbio.2006.11.015

Riva, S. C., Opara, U. O., & Fawole, O. A. (2020). Recent developments on postharvest application of edible coatings on stone fruit: A review. *Scientia Horticulturae, 262*, Article 109074. https://doi.org/10.1016/j.scienta.2019.109074

Santacruz, S., Rivadeneira, C., & Castro, M. (2015). Edible films based on starch and chitosan. Effect of starch source and concentration, plasticizer, surfactant's hydrophobic tail andmechanical treatment. *Food Hydrocolloids*, *49*, 89-94. https://doi.org/10.1016/j.foodhyd.2015.03.019

Sapper, M., Bonet, M., & Chiralt, A. (2019). Wettability of starch-gellan coatings on fruits, as affected by the incorporation of essential oil and/or surfactants. *LWT*, *116*, Article 108574. https://doi.org/10.1016/j.lwt.2019.108574

Serpa, A., & Vel, J. (2016). Vegetable nanocellulose in food science: A review. *Food Hydrocolloids 57*, 178-186. https://doi.org/10.1016/j.foodhyd.2016.01.023

Shih, Y. T., & Zhao, Y. (2021). Development, characterization and validation of starch based biocomposite films reinforced by cellulose nanofiber as edible muffin liner. *Food Packaging and Shelf Life*, *28*, Article 100655. https://doi.org/10.1016/j.fpsl.2021.100655

Silva, A. P. M., Oliveira, A. V., Pontes, S. M. A., Pereira, A. L. S., Souza Filho, M. de sá M., Rosa, M. F., & Azeredo, H. M. C. (2019). Mango kernel starch films as affected by starch nanocrystals and cellulose nanocrystals. *Carbohydrate Polymers*, *211*, 209-216. https://doi.org/10.1016/j.carbpol.2019.02.013

Soofi, M., Alizadeh, A., Hamishehkar, H., Almasi, H., & Roufegarinejad, L. (2021). Preparation of nanobiocomposite film based on lemon waste containing cellulose nanofiber and savory essential oil: A new biodegradable active packaging system. *International Journal of Biological Macromolecules*, *169*, 352-361. https://doi.org/10.1016/j.ijbiomac.2020.12.114

Soradech, S., Nunthanid, J., Limmatvapirat, S., & Luangtana-anan, M. (2017). Utilization of shellac and gelatin composite film for coating to extend the shelf life of banana. *Food Control*, *73*(Part B), 1310-1317. https://doi.org/10.1016/j.foodcont.2016.10.059

Soto-Muñoz, L., Palou, L., Argente-Sanchis, M., Ramos-López, M. A., & Pérez-Gago, M. B. (2021). Optimization of antifungal edible pregelatinized potato starch-based coating formulations by response surface methodology to extend postharvest life of 'Orri' mandarins Lourdes SotoMun. *Scientia Horticulturae, 288,* Article 110394. https://doi.org/10.1016/j.scienta.2021.110394

Stachowiak, N., Kowalonek, J., & Kozlowska, J. (2020). Effect of plasticizer and surfactant on the properties of poly(vinyl alcohol)/chitosan films. *International Journal of Biological Macromolecules*, *164*, 2100-2107. https://doi.org/10.1016/j.ijbiomac.2020.08.001

Sun, X., Wu, Q., Picha, D. H., Ferguson, M. H., Ndukwe, I. E., & Azadi, P. (2021). Comparative performance of bio-based coatings formulated with cellulose, chitin, and chitosan nanomaterials suitable for fruit preservation. *Carbohydrate Polymers*, *259*, Article 117764. https://doi.org/10.1016/j.carbpol.2021.117764

Syafri, E., Jamaluddin, Wahono, S., Irwan, A., Asrofi, M., Sari, N. H., & Fudholi, A. (2019). Characterization and properties of cellulose microfibers from water hyacinth filled sago starch biocomposites. *International Journal of Biological Macromolecules*, *137*, 119-125. https://doi.org/10.1016/j.ijbiomac.2019.06.174

Thakur, R., Pristijono, P., Golding, J. B., Stathopoulos, C. E., Scarlett, C. J., Bowyer, M., Singh, S. P., & Vuong, Q. V. (2018). Development and application of rice starch based edible coating to improve the postharvest storage potential and quality of plum fruit (*Prunus salicina*). *Scientia Horticulturae*, *237*, 59-66. https://doi.org/10.1016/j.scienta.2018.04.005

Thakur, Rahul, Pristijono, P., Scarlett, C. J., Bowyer, M., Singh, S. P., & Vuong, Q. V. (2019). Starch-based films: Major factors affecting their properties. *International Journal of Biological Macromolecules*, *132*, 1079-1089. https://doi.org/10.1016/j.ijbiomac.2019.03.190

Tibolla, H., Pelissari, F. M., Martins, J. T., Lanzoni, E. M., Vicente, A. A., Menegalli, F. C., & Cunha, R. L. (2019). Banana starch nanocomposite with cellulose nanofibers isolated from banana peel by enzymatic treatment: *In vitro* cytotoxicity assessment. *Carbohydrate Polymers*, *207*, 169-179. https://doi.org/10.1016/j.carbpol.2018.11.079

Ventura-Aguilar, R. I., Bautista-Baños, S., Flores-García, G., & Zavaleta-Avejar, L. (2018). Impact of chitosan based edible coatings functionalized with natural compounds on *Colletotrichum fragariae* development and the quality of strawberries. *Food Chemistry*, *262*, 142-149. https://doi.org/10.1016/j.foodchem.2018.04.063

Vieira, J. M., Flores-López, M. L., de Rodríguez, D. J., Sousa, M. C., Vicente, A. A., & Martins, J. T. (2016). Effect of chitosan-Aloe vera coating on postharvest quality of blueberry (*Vaccinium corymbosum*) fruit. *Postharvest Biology and Technology*, *116*, 88-97. https://doi.org/10.1016/j.postharvbio.2016.01.011

Widaningrum, W., Miskiyah, M., & Winarti, C. (2015). Edible coating berbasis pati sagu dengan penambahan antimikroba minyak sereh pada paprika: Preferensi konsumen dan mutu vitamin C [Sago starch-based edible coating with antimicrobial addition of lemongrass oil to peppers: Consumer preferences and vitamin c]. *Agritech Journal*, *35*(1), 53-60. https://doi.org/10.22146/agritech.9419

Xu, J., Xia, R., Zheng, L., Yuan, T., & Sun, R. (2019). Plasticized hemicelluloses/chitosan-based edible films reinforced by cellulose nano fiber with enhanced mechanical properties. *Carbohydrate Polymers*, *224*, Article 115164. https://doi.org/10.1016/j.carbpol.2019.115164

Yuan, Y., & Chen, H. (2021). Preparation and characterization of a biodegradable starch-based antibacterial film containing nanocellulose and polyhexamethylene biguanide. *Food Packaging and Shelf Life*, *30*, Article 100718. https://doi.org/10.1016/j.fpsl.2021.100718

Zhong, Y., & Li, Y. (2011). Effects of surfactants on the functional and structural properties of kudzu (*Pueraria lobata*) starch/ascorbic acid films. *Carbohydrate Polymers*, *85*(3), 622-628. https://doi.org/10.1016/j.carbpol.2011.03.031

Zhu, F. (2019). Food Hydrocolloids Recent advances in modifications and applications of sago starch. *Food Hydrocolloids*, *96*, 412-423. https://doi.org/10.1016/j.foodhyd.2019.05.035